AXISYMMETRIC FINITE ELEMENT ANALYSES OF THE KKP-II CONTAINMENT AND REACTOR PRESSURE VESSEL STRUCTURES

G. KOST, E.Y.W. TSUI

Engineering Decision Analysis Company, Inc., Palo Alto, California 94306, U.S.A.

N. KRUTZIK

Kraftwerk Union AG, D-6050 Offenbach (Main), Germany

SUMMARY

Two refined axisymmetric finite element models were used for the dynamic seismic analyses of the KKP-II Containment and RPV structures, using a postulated ground motion time history. One model was established primarily for the response of the containment structure, whereas the other was used for the response of the reactor pressure vessel plus internals.

In the first model, refined axisymmetric thin shell and solid elements were used for the containment components, while fluid elements were employed to represent the hydrodynamic effects of the fluid entrapped between the steel shells. Effects of the reactor building, RPV and internals, foundation mat, as well as soil-structure interaction are included, using equivalent cylindrical or solid elements and suitable classical solutions of rigid plates on infinite half space. Eigenvalues of the structure components of this model were generated and compared with those of similar but three-dimensional models established for KKP-I. The correlations were quite satisfactory.

In the second model, both refined beam and shell elements were used to represent the internals and pressure vessel, while fluid elements were used for the water contained within the RPV. Whenever hinged boundary conditions were encountered, the corresponding rotational degree of freedom was suppressed. Effects of the reactor building, concrete and steel containments, foundation mat and soil-structure interaction were likewise considered in this model, using relatively coarser equivalent finite elements. To solve the resulting consistent mass matrices efficiently, the determinant search eigenvalue extraction iterative technique was utilized.

The mode superposition procedure was used to generate most of the solutions of the present analyses, applying the recently updated digital program ASHSD3. For the purpose of determining the stress distributions within the internals more critically, a beam element and several special boundary conditions have been incorporated in this program. It now accepts four different types of elements, i.e., shell, solid, fluid and beam, and is capable of producing desirable force resultants and stresses, either by the isotropic beam theory or orthotropic shell or solid theory. To ensure the dynamic characteristics of the present models are accurate enough to provide meaningful response, eigenvalues and vectors of these models have also been compared with those of similar three-dimensional beam models. It was found that both results show good agreements, especially on the fundamental frequencies.

1. Introduction

This paper describes the seismic analyses of the containment and reactor pressure vessel structural systems for the KKP-II Nuclear Power Plant. Housed by the reactor building, the containment structure is composed of a steel shell which is partially filled with water, the projectile-protection concrete shells, the biological shield and the supporting concrete pedestals and walls; whereas the reactor pressure vessel system includes the fuel elements, shrouds, axial pumps, internal supporting grid structures, steam collectors and the boiling water. In the present analysis, it is assumed that both containment and the RPV systems have no restraints from the feed water, main steam and miscellaneous piping networks. The steel containment is composed of spherical, conical, cylindrical and plate sections, all of which are axisymmetrical in geometry, and all of the remaining structural components can be accurately approximated as such. It was determined that equivalent axisymmetric representations of the reactor building and a portion of the projectile-protection concrete shell, where irregular openings, columns and equipment penetrations axist, could be developed. To justify the use of the axisymmetric model for the present analyses, three axisymmetric representations of the structural components similar to the three-dimensional models used for KKP-I were developed prior to the establishment of the final two-dimensional model [4 - 6]. It was found that the dynamic characteristics of these axisymmetric models, especially the fundamental eigen frequencies, correlated very well with the three-dimensional models. Thus, a detailed and complete two-dimensional finite element model was developed and utilized in the analyses. The analyses were performed for the ground motions postulated for the Safe Shutdown Earthquake, and conducted in two basic steps, i.e., 1) evaluation of the dynamic characteristics and 2) generation of the dynamic response of the structure. The results of the analyses include undamped frequencies, mode shapes, displacements, accelerations, floor response spectra, and stresses at selected locations.

2. Idealization of Structural Components

Structural components which were considered in the mathematical model are thin-walled shell elements, thick-walled shell or solid components, irregular structural elements, such as columns and walls with openings, fuel element supporting grids, etc., effective shell and beam elements such as fuel rods, CRD tubes and housing, etc., and equivalent shell and solid elements such as reactor building and soil springs. Formulations of stiffness matrices for most of the finite elements under consideration have been described in references [1 - 3].

2.1 Thin-Walled Shell Components

Regular shell elements are used for both thin-walled steel and concrete members, including the stiffeners attached to the inner cylinder, lower cone and sphere of the steel containment. Such elements have four degrees of freedom at each nodal point, and their thickness may vary linearly along the element axial direction. The average thickness is used for the integration of the lumped masses at the nodal points. Except for the cases of transformed sections such as the elements used for the reactor building, this type of element is utilized when the radius to thickness ratio of the element is large. In the case of hinge boundary conditions, the corresponding rotational degree of freedom is appropriately suppressed.

2.2 Thick-Walled Shell and Solid Components

When the ratio of radius to thickness of the member is considerably less than 10, such as the case for the concrete supporting ring and foundation mat of the reactor building, quadrilateral or triangular elements are used in the analysis. For these elements, shear deformations are included in the formulation of the element stiffness matrix, and the stresses produced within the element are constant.

2.3 Irregular Structural Components

For the concrete-filled steel columns, fuel rods and their associated components, beam elements are used, and for steel grids, concrete walls with cutouts and other nearly axisymmetric concrete members, equivalent shell elements are provided. The latter can be established either by the reduction of the modulus of the materials [5] or the modification of the moment of inertia of the cross-section of the member. In either case, the element mass density is adjusted to retain the dynamic similarity between the actual and the equivalent member.

3. Structure-Soil Interaction

The effects of structure-soil interaction may be represented either by equivalent solid or cylindrical elements. To achieve this, it is desirable to evaluate the appropriate values for the constants of the horizontal spring k_{xx}, rocking spring $k_{\phi\phi}$, vertical spring k_{zz}, including the coupling spring between the horizontal and rocking $k_{x\phi}$ [7 - 10]. Once these soil spring characteristics are known, the geometric and material properties of the equivalent structural elements can be determined as follows:

3.1 For Horizontal Earthquake Excitations:

If shear deformations are included, the total length (L), moment of inertia (I) and modulus of elasticity (E) of the massless cantilever element are governed by the following expressions:

$$L = 2k_{x\phi}/k_{xx} \tag{1}$$

$$I = (AC/6)[(3k_{\phi\phi}/k_{xx}) - (2k_{x\phi}/k_{xx})^2] \tag{2}$$

and $$E = \frac{[1 + (24I/ACL^2)]L}{[4 + (24I/ACL^2)]I}\, k_{\phi\phi} \tag{3}$$

where A and C are the cross-sectional area and the shear factor, respectively. It is apparent that eqs. (2) and (3) are implicit because the value of A has to be assumed first. If solid elements are used, however, this difficulty can be eliminated since the quantities A and I can be expressed in terms of the radius (R) of the cross-section, and consequently eqs. (2) and (3) can be transformed into the following form:

$$R = \sqrt{(2C/3)[(3k_{\phi\phi}/k_{xx}) - (2k_{x\phi}/k_{xx})^2]} \tag{4}$$

$$E = \frac{4L[1 + (6R^2/CL^2)]}{\pi R^4[4 + (6R^2/CL^2)]}\, k_{\phi\phi} \tag{5}$$

The basic assumption used for the derivation of eqs. (1) through (5) is that the horizontal springs are coupled with those for rocking.

3.2 For Vertical Earthquake Excitations:

When an axisymmetric structure is subjected to seismic motions in the Z-direction, it is logical to consider that only the vertical spring k_{zz} is acting, and the equivalent cross-sectional area can be determined from the following expression:

$$A = k_{zz}L/E \tag{6}$$

where L and E are given by eqs. (1) and (3) or (5), respectively.

4. Evaluation of the Hydrodynamic Effects

Since the reactor pressure vessel and the steel containment are partially filled with fluid, the hydrodynamic effects on both dynamic characteristics and response of the system must be properly considered in seismic analyses. In essense, both apparent and virtual hydrodynamic masses are induced physically by the force which an immersed accelerating solid must impart to the fluid in order to cause it to accelerate. Such force should be distinguished from the drag force because the former is acceleration dependent whereas the latter relies on velocity. To obtain a consistent hydrodynamic mass matrix for a fluid element, the following assumptions are postulated:

- the fluid is incompressible and invicid
- vertical velocity vector component is zero
- the horizontal velocity field is linear
- the fluid is entrapped in concentric flexible cylindrical shells
- leakages of fluid through the cylinders are permissible

Accordingly, the desired mass matrix can be derived through the minimization of the kinetic energy of the solid-fluid system, using the following Euler-Lagrange equation of motion:

$$\frac{d}{dt}\frac{\partial T}{\partial \dot{u}} - \frac{\partial T}{\partial u} - \frac{\partial V}{\partial u} = Q \tag{6}$$

where T, V, u, $\dot{u}$ and Q are the kinetic energy, strain energy, generalized displacement, velocity and force vectors, respectively.

Based on the above assumptions and using only the first term of the Fourier expansion of the velocities, it can be shown that the kinetic energy of the system can be approximated by the following expression if the higher order velocity terms are disregarded

$$T = \frac{M}{4}\left\{\underline{\dot{u}}_r^2 + \underline{\dot{u}}_\theta^2 - K\underline{\dot{u}}_\theta\left[\left(\dot{u}_r^j + \dot{u}_r^k\right) - \left(\dot{u}_r^i + \dot{u}_r^l\right)\right]\right\} \tag{7}$$

where $K = \frac{\alpha}{\beta - 1}$ = a parameter

α = Leakage factor

β = Ratio of the radii of the outer vertical face "kl" to the inner face "ij" of the element having nodal points "ijkl" [3]

$\underline{\dot{u}}_r(\underline{\dot{u}}_\theta)$ = Mean radial (tangential) velocity of the element

$\dot{u}_r^\gamma(\dot{u}_\theta^\gamma)$ = Radial (tangential) velocity of nodal point γ, γ = i, j, k, l

and M represents the total apparent mass of fluid entrapped by the vertical faces of the element. It is of interest to note that there are coupling terms involved between the nodal radial velocities and the mean tangential velocity in eq. (7) which render the resulting mass matrix with off-diagonal terms. Recalling that the fluid is incompressible, i.e., V=0, and for undamped free vibrations, $Q=\partial T/\partial u=0$, the desired mass matrix (M) can be obtained simply by differentiating the kinetic energy given by eq. (7) with respect to the generalized velocity and time [11]:

$$\frac{d}{dt}\frac{\partial T}{\partial \dot{u}} = M_{mn}\ddot{u} \qquad m, n = 1, 2, 3...8 \tag{8}$$

Since there are two velocity components for each nodal point, the order of the resulting symmetric banded mass matrix is mxn=8x8.

It should be noted that the fluid elements are introduced for the dynamic analyses for Fourier harmonic n=1 and under horizontal earthquakes only. For vertical ground excitations (n=0), the masses of fluid are lumped at nodal points.

5. Mathematical Models

The mathematical models established for the Containment and Reactor Pressure Vessel systems are shown in Figures 1 and 2, respectively. The first model has 151 nodes, 180 elements and approximately 600 dynamic degress of freedom. Element Number 1 represents the effects of structure-soil interaction. Due to the limitations of the applicability of the fluid elements, they are used only for the top layers of the water entrapped in the steel shells and solid elements with negligibly small stiffness are introduced for the lower portion of the fluid. Since this model is intended for the Containment structures, both stiffnesses and masses of the internals, shrouds, etc., including the fluid contained in the RPV, are added to the elements located along the cylindrical portion of the pressure vessel. The second model consists of 111 nodal points 146 elements and about 430 degrees of freedom. Emphasis is on the response of the RPV and Internals for this model; therefore, only two-mass subsystems are introduced for other structural components such as the biological shield, containments and reactor building. The effects of structure-soil interaction are represented by three solid elements (Element Numbers 140, 141 and 142). Generally, the stiffness matrices are coupled vertically whereas the mass matrices, especially for the fluid elements, are coupled horizontally, and hence horizontal numbering patterns of the nodal points are adopted to minimize the band widths of both stiffness and mass matrices.

6. Dynamic Response

Because of the limitation of time on meeting the paper deadline, preparation of input data for the dynamic analysis of the RPV and Internals system was still under way while this manuscript was being written. Consequently, only the results of the dynamic analysis of the Containment System (see Figure 1) are presented and discussed. However, results of the dynamic response for the RPV and Internals Model will be reported in Reference [11] at a later date. The modal superposition time-history technique was used in the analysis. Values of the modal damping were evaluated by the energy method [2, 12]. A maximum value of 20 per cent was used. The forcing function used for the horizontal ground ground excitations is depicted in Figure 3. In the case of vertical excitations, 50 percent of the amplitude of this 10-second artificial ground acceleration time history was applied.

Prior to the time-history analysis, several response spectrum analyses were conducted, using appropriate ground response spectra supplied by KWU [2, 6]. The results of such spectrum analyses reveal that the response is primarily contributed by the first seven modes for both Fourier harmonics n=0 and n=1. In order to generate accurate results, however, a maximum number of ten modes was used in the time-history analyses. To carry out numerically the stepwise time integrations involved, the mid-point acceleration algorithm was employed, using a time step (Δt) of about 0.014 second [1].

Due to the space limitation, only the results for the horizontal earthquake (n=1) are briefly reported herein. These results are based on a value of shear modulus of soil, $G=3\times10^4$ Mp/m^2. Table 1 shows the dynamic properties of the Containment Model. Table 2 shows the absolute maximum values of the absolute accelerations at 27 selected nodal points (see Fig. 1). The absolute maximum values of the relative displacements for both concrete and steel containments are shown in Figure 4, and the floor response spectra for a representative location (Nodal Point 146) are depicted in Figure 5.

In view of the amplitudes of the absolute accelerations for various control points listed in Table 2, it is apparent that the accelerations are dominated by the radial components as expected, with a maximum value of 1.694 m/s^2 at Nodal Point 146. The absolute maximum relative displacements for the systems under consideration shown in Figure 4 occurred almost instantaneously at t=5.769 seconds. It can be observed that the motions for both concrete and steel containments are essentially in phase at this particular time. This does not mean that they are vibrating in a similar manner during the entire period of the ground excitations [13]. According to the time-history of response, the motions of both the inner cylindrical and spherical components of the steel containment around the top layer of the fluid are always in phase and the absolute maximum difference of velocities between these components is small. Therefore, hydrodynamic effects on the actual response of the steel shells are insignificant. The stresses in the steel containment are relatively low. For example, the maximum meridional stress at the lower portion of steel shell near the juncture of steel and concrete sections is approximately 1000 Mp/m^2.

References

[1] Ghosh, S., and Wilson, E., "Dynamic Analysis of Axisymmetric Structures under Arbitrary Loading," EERC 69-10, University of California at Berkeley (September 1969).

[2] EDAC, "Summary of Criteria and Procedures for Extreme Load Dynamic Analyses of Structures for the KKP-II Nuclear Power Plant," Technical Report No. EDAC-101.01, Engineering Decision Analysis Company, Inc., Palo Alto, California (1975).

[3] Tsui, E. Y. W., "Axisymmetric Reactor and Internals Model for Seismic Analyses," Paper No. K6/9, 2nd International Conference on Structural Mechanics in Reactor Technology, Berlin, Germany (September 1973).

[4] Krutzik, N., "Dynamische Berechnungen der Reaktoranlage KKP-I, Teil I, Idealisierung der Struktur," Technicher Bericht Nr. AEG-E3-2384 (September 1972).

[5] Krutzik, N., "Dynamische Berechnungen des Sicherheitsbehälters KKP-I, Technischer Bericht Nr. KWU-E3-2820 (October 1973).

[6] Krutzik, N., "Dynamische Bereschnungen von Unterstrukturen der Anlage KKP-I, 2. Sicherheitsbehälter," Technischer Bericht, KWU-R2-3010 (August 1974).

[7] Novak, M., "Effect of Soil on Structural Response to Wind and Earthquake," *Earthquake Engineering and Structural Dynamics*, 3, pp. 79-96 (1974).

[8] Novak, M., and Sachs, K., "Torsional and Coupled Vibrations of Embedded Footings," *Earthquake Engineering and Structural Dynamics*, 2, pp. 11-33 (1973).

[9] Whitman, R. V., and Richart, F. E., "Design Procedures for Dynamically Loaded Foundations," *Journal of the Soil Mechanics Division*, ASCE (November 1967).

[10] Richart, F. E., et al, *Vibrations of Soils and Foundations*, Prentice-Hall, Inglewood Cliffs, N. J. (1970).

[11] EDAC, "Dynamic Seismic Analyses of the Reactor Pressure Vessel and Internals for the KKP-II Nuclear Power Plant," Technical Report No. EDAC-101.05, Engineering Decision Analysis Company, Inc., Palo Alto, California (1975).

[12] Ragett, J. D., "Estimating Damping of Real Structures," ASCE National Conference, 1974.

[13] EDAC, "Dynamic Seismic Analysis of the Containment Structure for KKP-II Nuclear Power Plant," Technical Report No. EDAC-101.04, Engineering Decision Analysis Company, Inc., Palo Alto, California (1975).

K 6/2

TABLE 1

DYNAMIC PROPERTIES OF THE CONTAINMENT SYSTEM (n=1)

MODE NO.	EIGEN FREQUENCY (cps)	DAMPING RATIO (critical)	MODAL PARTICIPATION (percent)
1	1.548	0.200	56.428
2	3.850	0.100	6.251
3	5.406	0.200	30.932
4	6.572	0.065	4.206
5	7.208	0.051	0.834
6	10.560	0.054	1.225
7	12.160	0.050	0.045
8	13.253	0.050	0.013
9	15.745	0.050	0.036
10	15.832	0.050	0.029

TABLE 2

ABSOLUTE MAXIMUM VALUES FOR TOTAL ACCELERATION

NP	TIME	R-ACCEL	TIME	Z-ACCEL
7	4.298E+00	-1.058E+00	4.270E+00	-1.713E-01
13	5.726E+00	9.816E-01	4.255E+00	-2.994E-01
15	4.298E+00	-1.012E+00	4.255E+00	-1.980E-01
22	5.726E+00	9.924E-01	4.255E+00	-3.259E-01
44	5.726E+00	9.932E-01	4.255E+00	-2.766E-01
51	5.726E+00	9.881E-01	4.255E+00	-3.743E-01
52	5.726E+00	9.771E-01	4.255E+00	-6.174E-01
54	5.726E+00	9.927E-01	4.255E+00	-2.009E-01
57	5.726E+00	9.706E-01	4.255E+00	-4.667E-01
65	5.726E+00	9.822E-01	4.255E+00	-5.905E-01
74	5.726E+00	9.961E-01	4.255E+00	-2.221E-01
78	5.726E+00	9.924E-01	4.255E+00	-4.728E-01
83	5.726E+00	9.946E-01	4.255E+00	-3.360E-01
91	5.726E+00	9.867E-01	4.255E+00	-3.466E-01
107	2.242E+00	1.035E+00	4.270E+00	-3.719E-01
114	5.741E+00	1.027E+00	4.255E+00	-3.721E-01
115	5.741E+00	1.063E+00	4.255E+00	-9.724E-01
116	3.441E+00	1.244E+00	4.255E+00	-2.579E-01
117	3.898E+00	-1.090E+00	4.255E+00	-1.981E-01
118	2.242E+00	1.180E+00	4.270E+00	-3.785E-01
122	2.470E+00	1.091E+00	4.255E+00	-3.836E-01
132	3.441E+00	1.503E+00	4.255E+00	-2.618E-01
134	2.242E+00	1.363E+00	5.940E+00	9.114E-01
136	2.470E+00	1.276E+00	4.255E+00	-8.894E-01
141	5.812E+00	1.597E+00	5.940E+00	6.012E-01
144	2.485E+00	1.597E+00	4.255E+00	-5.662E-01
146	5.826E+00	1.694E+00	5.940E+00	3.303E-01

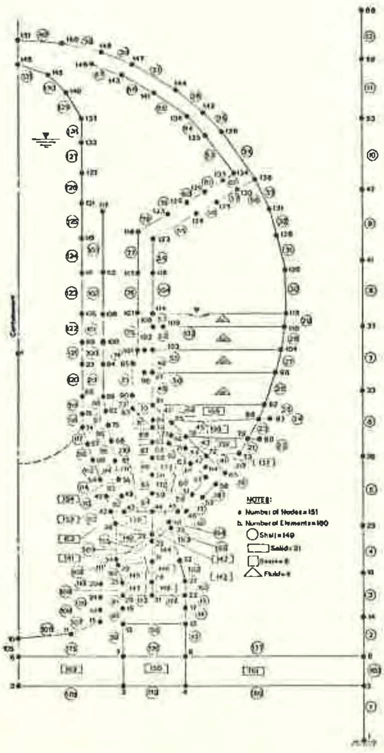

FIGURE 1 MATHEMATICAL MODEL FOR THE CONTAINMENT SYSTEM

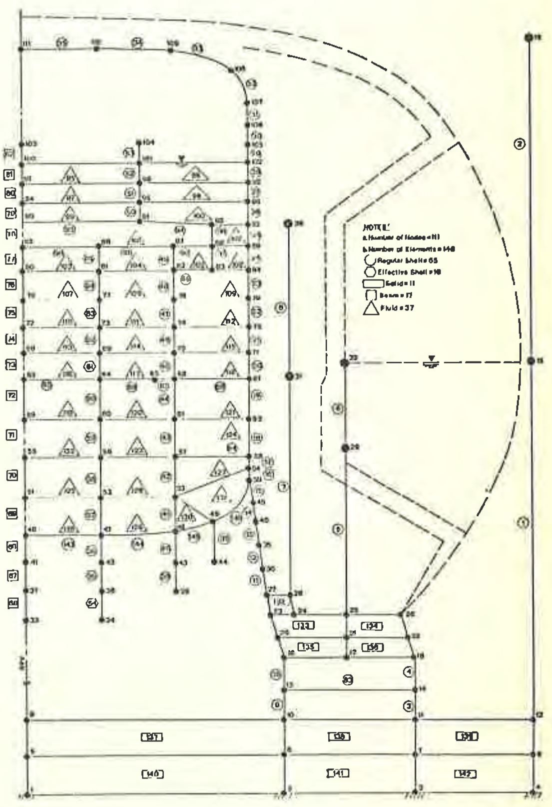

FIGURE 2 MATHEMATICAL MODEL FOR THE RPV SYSTEM

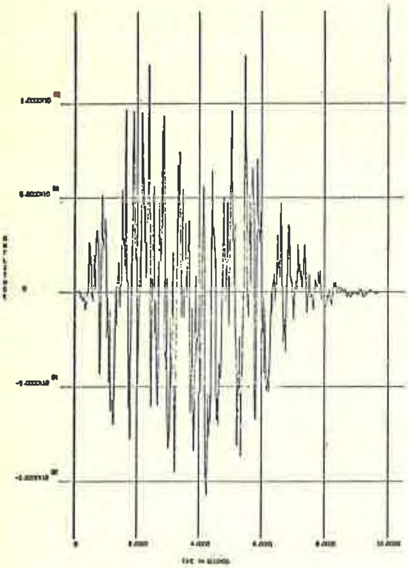

FIGURE 3 FORCING FUNCTION

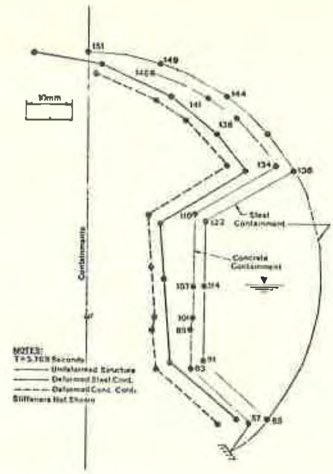

FIGURE 4 RELATIVE DISPLACEMENTS FOR THE CONTAINMENTS

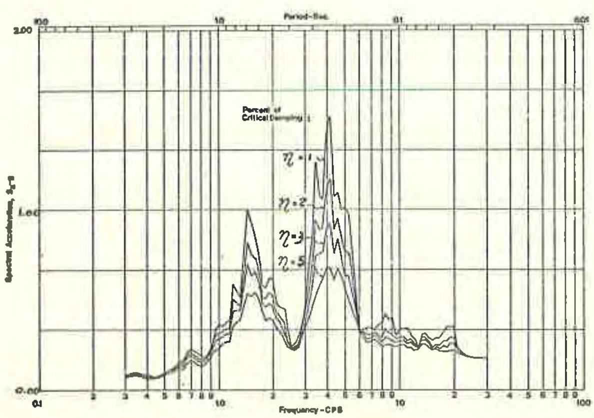

FIGURE 5 FLOOR RESPONSE SPECTRA FOR NODAL POINT 146